PROGRESS IN COLOR, COLORANTS AND COATINGS

available online @ www.pccc.icrc.ac.ir

Prog. Color Colorants Coat. 15 (2022), 1-9

Ministry of Science, Research and Technology
Institute for Color Science and Technology

Studying the Active Corrosion Inhibition Effect of the Ce^{3+}/2-Mercaptobenzothiazole Loaded NaY Zeolite/Zn-Al LDH Based Containers in a Silane Coating

P. Kardar*, R. Amini

Department of Surface Coatings and Corrosion, Institute for Color Science and Technology (ICST), P.O. Box: 16765-654, Tehran, Iran.

ARTICLE INFO

Article history:
Received: 01 Oct 2019
Final Revised: 25 Apr 2020
Accepted: 28 Apr 2020
Available online: 31 Jan 2021

Keywords:
Corrosion
Self-healing
Nano-containers
Inhibitors
Layered double hydroxides (LDHs)
EIS.

ABSTRACT

In the present study, the corrosion protective ability of the sol-gel based composite coatings containing two-different types of the cationic/anionic based inhibitors loaded containers. For this purpose, the NaY zeolite and Zn-Al Layered double hydroxides (LDHs) containers were loaded with Ce^{3+} cations and 2- mercaptobenzothiazole (MBT) separately. The morphology and composition of the constructed micro/nanocontainers were studied using analytical methods, confirming the successful loading of the inhibitors. In this study, the Ce^{3+}/MBT inhibitors were successfully introduced into the LDH/NaY-based zeolite containers. Results evidenced that the combination of the two inhibitors has a constructive effect on the active protection of the AA2024-T3 sheets. SEM micrographs of the unfilled LDH and stupefaction with MBT show that the prepared LDHs have sheet-like morphology. The addition of single-inhibitor filled containers to the sol-gel hybrid coating, and water-based epoxy coating provided active protection for the AA2024-T3 coated substrate. However, the combination of the filled containers with the inhibitor in the above-mentioned coatings resulted in the improvement of the active protection of the substrate, which confirms the synergy between the particles. The NaY containers loaded with the Ce^{3+} resulted in a significant increase of the $|Z|_{0.01\ Hz}$ of the gel-sol hybrid coatings, which indicates the formation of a stable oxide layer with higher resistance. Whereas the $|Z|_{0.01\ Hz}$ of the hybrid sol-gel coatings loaded with LDH-MBT were in the same range as the NaY-Ce loaded coatings, containing NaY-Ce and LDH-MBT, showed the highest $|Z|_{0.01\ Hz}$ values that indicate the synergy between the inorganic (Ce^{3+}) and organic (MBT) inhibitors in sol-gel hybrid coatings. Prog. Color Colorants Coat. 15 (2022), 1-9© Institute for Color Science and Technology.

1. Introduction

Passive protective coatings are one of the most common corrosion protection methods of metal substrates. Their protective mechanism is based on the retardation effect of the coatings against the entry of water and corrosive species to the coating-metal interface [1, 2]. However, after mechanical damage, these coatings do not show adequate protective performance, but adding corrosion inhibitors to the

*Corresponding author: * kardar@icrc.ac.ir

coating formulation can create extrinsic self-healing properties [3].

Despite the development of multifunctional inhibitors, their direct addition to the coating formulations can lead to inevitable problems such as chemical interactions between the inhibitor and the polymer matrix follows by the degradation of the coating and the loss of inhibitor activity. Encapsulation of the corrosion inhibitors in neutral host structures, which is called micro/nano container, not only can separate the active agents from the coating components but also control the release of the inhibitors. Recently, the zeolite and clay-based particles have attracted much attention because of their ion exchangeability and high loading capacity, as the host structures for corrosion inhibitors [4, 5].

Zeolites are microporous aluminosilicate crystals with a negative surface charge. This negative charge is neutralized by the cations that attached to their bodies [6, 7]. Active cationic species such as cerium and lanthanum ions can be trapped inside the structural cages of zeolite particles through the cation exchange process. The inhibitors trapped in these containers are stimulated and released by corrosion activities, including pH changes and the presence of cationic species (Mn^+ and H^+).

Selective release of the inhibitor ions from the damaged site can strengthen the protective oxide layer, and as a result, it guarantees long-term protection for the metal substrate. The combination of zeolites loaded with Ce^{3+} and La^{3+} inhibitors in corrosion protection coatings results in active protection improvement as a result of the synergy between these two types of inhibitors [8]. Organic-inorganic hybrid coatings containing such vehicles had a significant improvement in the active protection of substrates such as AA2024 compared to those loaded with zeolites containing single inhibitors [9, 10].

LDHs are a class of anionic exchangeable clay particles that consist of linked metal hydroxide layers with a positive charge. The positive charge of these structures compensated by the placement of anionic species between the hydroxide layers [11, 12]. The LDH particles with inhibitor can limit their release to corrosion activating phenomena such as changes in pH or the presence of released anions resulting from the corrosion processes. Successful entrapment of anionic inhibitors in LDH has been reported in the literature [13, 14]. Tedim et al. report the synthesis of layered double hydroxides (LDHs) nanocontainers loaded with different corrosion inhibitors (vanadate, phosphate, and 2-mercaptobenzothiazolate) and the characterization of the resulting pigments by X-ray diffraction (XRD) and transmission electron microscopy (TEM). The anticorrosion activity of these nanocontainers with respect to aluminum alloy AA2024 was investigated by electrochemical impedance spectroscopy (EIS). The results show that an enhancement of the active protection effect can be reached when nanocontainers loaded with different inhibitors are combined in the same protective coating system [14]. In 2009, the anticorrosion capabilities of LDHs loaded with organic inhibitors toward the AA2024 aluminum alloy were analyzed by electrochemical impedance spectroscopy. A significant reduction of the corrosion rate is observed when the LDH nanopigments are present in the corrosive media. The mechanism by which the inhibiting anions can be released from the LDHs underlines the versatility of these environmentally friendly structures and their potential application as nanocontainers in self-healing coatings [13].

Although the synergistic effect of the anionic inhibitors that have been separately introduced into LDH inter-layer space [15], a few research has been done on the synergistic effect of the cationic and anionic inhibitors filled containers.

In the present study, the corrosion protection coatings were prepared and evaluated with an extrinsic self-healing feature containing a combination of containers with cationic and anionic inhibitors. For this purpose, NaY zeolite and Zn-Al LDH with Ce^{3+} and 2-mercaptobenzothiazole were selected as cationic and anionic inhibitors, respectively. The morphology and composition of the constructed nanocontainers were studied using analytical methods that confirm the successful loading of the inhibitors used. Furthermore, sol-gel and water-based epoxy extrinsic healing coating containing individual inhibitor filled containers, as well as their combination, were prepared and evaluated using bulk and local electrochemical characterization techniques.

2. Experimental

2.1. Materials

Pure AA2024-T3 aluminum alloy with composition of Al=94.5, Fe=0.5, Cu=4.9 and Cr=0.1 (weight percentage) used as a metal substrate. Zirconium

propoxide (70 wt% in n-propanol with a molecular weight of 327.57 g/mol), 3-glycidoxypropyl trimethoxy silane (with a purity of over 98 % and a molecular weight of 326 g/mol), that labeled as TPOZ and GPTMS, respectively, and ethyl acetoacetate (with purity over 99 % and molecular weight of 130.14 g/mol) were purchased from Sigma-Aldrich Co., and then, they were used to prepare sol-gel coatings without any manipulation. Cerium (III) nitrate hexahydrate (with purity over 99 % and molecular weight of 342.22 g/mol), 2-mercaptobenzothiazole (with purity over 97 % and molecular weight of 167.25 g/mol) that called as MBT, were purchased from Sigma-Aldrich and used as a corrosion inhibitor without further purification. Y zeolite (with a molar ratio of 5:1 of silicon dioxide to aluminum oxide and 13 wt% sodium oxide) was purchased from Focus-Zeolite Company.

2.2. Preparation of NaY zeolite and LDH nanocontainers

The Y zeolite with a single inhibitor was prepared by the exchange of Na^+ cations in the Y zeolite cages with Ce^{3+} cations. The ionic exchange procedure was performed in the $CeNO_3$ aquatic solution with Ce^{3+} over 300% related to the cation exchange capacity of Y zeolite to maximize the exchange of Na^+ ions with Ce^{3+} inhibitors. The exchange process was performed by adding NaY zeolite to 0.3 M $CeNO_3$ solution at a volume/particle ratio of 20 mL/g at 60 °C. NaY zeolite with Ce^{3+} that is named NaY-Ce was washed and filtered and then dried at 60 °C for 24 hours. Finally, the NaY zeolite powder with 12 % weight of Ce^{3+} was obtained.

The preparation of Zn-Al LHD with an inhibitor has two main steps: (1) Synthesis of LDH precursors and (2) The substitution of the inorganic anions with MBT inhibitor anions during the ion exchange reaction. The synthesis was carried in the presence of the argon, and all solutions were prepared by distilled water to prevent the contamination with carbonate anions. The molar ratio of zinc to aluminum was 2:1 to obtain stable compounds.

In the first step, 0.5 M of Zn $(NO_3)_2$-$6H_2O$ and 0.25 M of $Al(NO_3)_3$-$9H_2O$ solution (50 mL) was slowly added to 1.5 M $NaNO_3$ (100 mL, pH=10) under severe stirring at room temperature. During this reaction, the pH was kept constant (pH=10) by adding 2 M NaOH simultaneously. After that, the heat treatment was performed on the obtained slurry at 65 °C for 24 hours to crystallize the LDHs; subsequently, the mixture was centrifuged, and the obtained product was washed 4 times with distilled water.

The anion exchange reaction was carried out by dispersing the LDH precursors in an aqueous solution containing organic anions more than twice. The MBT sodium salts were previously prepared by neutralizing the MBT aqueous solutions with an equivalent amount of aqueous NaOH. After that, the gel-like and white LDH precursors were dispersed in 0.1 M NaMBT solution (pH = 10) under the argon atmosphere. The total amount of this solution (120 mL) was divided into two 60 mL portions. The LDH precursors were added to one of these portions and then centrifuged. This procedure was repeated with the second part of the organic anionic solution. Finally, the LDH powders containing organic anion were washed four times with distilled water, frozen, and then dried at -78 °C by freezing [13, 14].

2.3. Characterization

The morphology of the nanocontainers was studied with an LEO SEM device with an acceleration voltage energy of 10 kV. In addition, the composition of the containers loaded with inhibitors and those without inhibitors was studied by X-ray diffraction (EDS) spectroscopy at 15 kV. LDH nanocontainers structure with inhibitor and LDH nanocontainers structure without inhibitor was investigated by X-ray diffraction (XRD) test. The tests were performed using a Philips X'Pert diffractometer with Cu Kα radiation source.

2.4. Preparation of coating

Before applying the coating, the AA2024-T3 panels with a dimension of 3×4 cm^2 were mechanically ground with silicon carbide paper with 1000 mesh, and then the samples were degreased in ethanol for 5 min. Then the sheets were immersed in 2M NaOH solution for 10 seconds and washed with distilled water to increase the surface density of the hydroxyl (OH^-) groups on the AA2024-T3 substrate. The cleaned and dried sheets of AA2024-T3 were covered with two types of coatings: 1) SiO_2-ZrO_2 sol-gel hybrid coating and 2) water-based epoxy coating.

Sol-gel coatings: Hybrid sols were prepared by mixing two different sols through hydrolysis of TPOZ and GPTMS n n-propanol. Silane based sol was

prepared by dropwise addition of 0.33 M of acidic deionized water with pH = 0.5 to GPTMS solution containing 1 M of n-propanol. Pre-hydrolysis was performed by stirring the mixture at 300 rpm for 1h at room temperature.

Zirconia-based sol was prepared by mixing TPOZ (70 wt.% in n-propanol) and ethyl acetoacetate in a 1:1 volume ratio at room temperature for 20 min. The pre-hydrolysis was performed by adding 2.62 M of acidic deionized water with pH = 0.5 to the mixture, and the solution was stirred at room temperature for 1 hour [15].

The Pre-hydrolyzed sols were mixed using a magnetic stirrer for one hour. After that, the sol-gel hybrid solution was applied to the AA2024-T3 sheets. 10% wt of micro/nanocontainers with and without inhibitors were added to the sol-gel hybrid solution in the mixing step of TPOZ and GPTMS sols. The cleaned AA2024 sheets were immersed in a sol-gel hybrid solution for 100 s and then came out at a rate of 18 cm/min. The coated samples were dried at ambient temperature for 30 min, and then the samples with a mean thickness of 4±2 μm were prepared by a two-step baking process at 60 and 120 °C for 80 minutes.

The epoxy coating formulation includes a water-based epoxy emulsion and a solvent-free amine hardener. Before adding harder to the formulation, 10 % wt of pigment (i.e., micro and nanocontainers) was added to the resin, and it was mechanically stirred at 1000 rpm for 5 minutes to ensure full pigment dispersion in the resin. Hardener was then added to the mixture with a weight ratio of resin to hardener of 0.7:1, and then it was mechanically stirred. In the next step, the resulting mixture was cast onto the cleaned AA2024-T3 sheets using a rod-like coater with 50 μm thickness. The coated samples were cured at room temperature for 72 h. Finally, the coatings with an average dry thickness of 30 μm were obtained.

2.5. Characterization of the coatings

The electrochemical properties of the coatings prepared were studied by the EIS method. EIS measurements were performed at room temperature on a three-electrode cell (Calomel electrode (SCE), a Pt auxiliary electrode, and the coated samples). The aqueous solution of 3.5 wt% sodium chloride was used as the test electrolyte. This test was performed using an Ivium compact stat machine with a scanning rate of 1 mV/s in a potential perturbation range of ±200 mV compared with open circuit potential. Moreover, the uncoated AA2024-T3 panels were tested using EIS on electrolytes containing $CeNO_3$ and MBT at different molar ratios. The electrolytes were prepared using an aqueous solution of 3.5% sodium chloride as a base solution. The molar ratio of Ce: MBT was changed as follows: 1: 99, 90:10, 75:25, 50:50, and 25:75.

3. Result and Discussion

3.1. Morphological analysis of the constructed containers

The composition of the NaY zeolites and Ce-filled NaY zeolites were investigated using SEM/EDS analyses (Figure 1). SEM micrographs related to the NaY and NaY-Ce particles show specific crystals with an average diameter of fewer than 1 μm. The EDS profile of the NaY shows a particular peak at 1.04 kV that is related to Na^+ cations present in Y zeolite cages. Replacement of Na^+ cations with Ce^{3+} cations in the NaY can be confirmed by the significant decrease in Na^+ (from 9.6 wt% to 3.1 wt %), and the appearance of Ce characteristic peaks at 4.84, 5.27, 5.60 and 6 kV. The presence of Na characteristic peak in the EDS spectrum of NaY-Ce indicates an incomplete exchange process. The incomplete exchange of Na^+ with Ce^{3+} cations in NaY-Ce can be attributed to the size limitation of the sodalite cages for placement in the Ce hydrated cations [16]. The elemental analysis of NaY-Ce particles with EDS showed successful loading of 12 wt% Ce in Y zeolite.

The structures of LDH nanocontainers filled with inhibitor were evaluated by XRD (Figure 2). The XRD pattern of LDH nanoparticles (interlayer with NO_3^- anions) showed distinct peaks at 9.86, 19.92, and 30°, which correspond to the (003), (006), and (009) reflections, respectively. The interlayer space height was calculated based on the cation sheet thickness (0.477 nm) and the interlayer d-spacing (0.9 nm), and the value was 0.42 nm. The calculated gallery height is in good agreement with the NO_3^- (0.38 nm) anion size. The slight difference in the amount of the obtained and the diameter of the NO_3^- anion can be justified by the vertical alignment of the NO_3^- groups relative to the host layer.

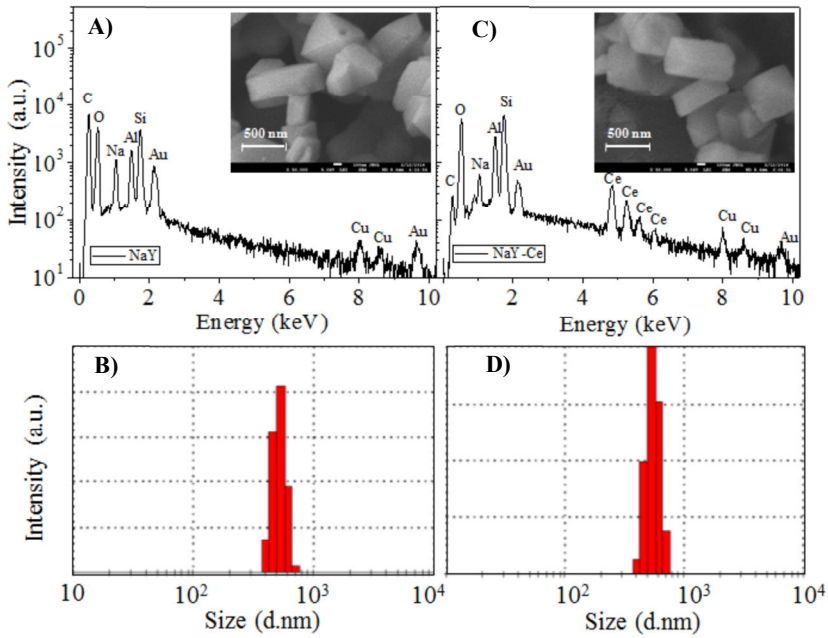

Figure 1: SEM and EDS images of the composition of non-filled NaY zeolites (A and C) and Ce-loaded NaY zeolites (B and D).

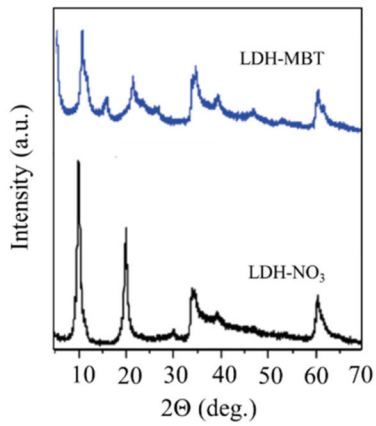

Figure 2: XRD patterns related to the LDH nanocontainers loaded with inhibitor MBT.

Substitution of NO_3^- by MBT anions through anion exchange process leads to the structural changes that are characterized by changes in the position of the peaks towards the few 2θ angles, and their intensity decreases sharply. The new peak position corresponds to the 1.72 nm interlayer distance, which is compatible with the relatively larger size of the interlayer anions, i.e., MBT.

The structure of Zn-Al LDHs filled with/without MBT was evaluated by SEM. SEM micrographs of the unfilled LDH (Figure 3A) and stupefaction with MBT (Figure 3B) show that the prepared LDHs have sheet-like morphology that preserved by anion exchange, as reported in literature [13].

3.2. Active corrosion protection properties of the coatings

To evaluate the active inhibition performance of the containers modified with Ce^{3+} and MBT, a number of water-based coatings containing 10 wt% NaY, 10 wt% NaY-Ce, 10 %wt LDH-MBT, and 5% wt NaY-Ce + 5% LDH-MBT were prepared, respectively. The active protection provided by the inhibitors filled containers, were evaluated by the creation of two circular defects with an average diameter of 150 µm, reaching the metal substrate.

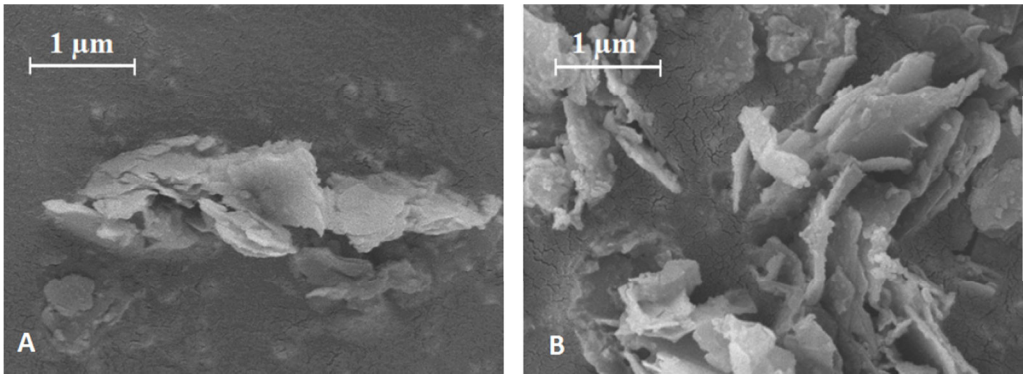

Figure 3: SEM images of the pure (A) and MBT filled (B) Zn-Al LDHs (A).

The Bode plots at the early stages of measurement and the low-frequency ($|Z|_{0.01\ Hz}$) frequencies of the SiO_2-ZrO_2 hybrid (Figure 4A and 4C) and water-based epoxy (Figure 4B and 4D) are presented in Figure 4. In the early stages of measurement, the EIS spectra of the SiO_2-ZrO_2 hybrid coatings (Figure 4A) showed two-time constants in the test frequency range, which corresponds to the response of the coating and oxide layer. After long-term exposure to the electrolyte, a third-time constant, which is attributed to corrosion occurrence at the metal surface, was observed in the EIS spectra of the coated systems [17].

The coating loaded with NaY particles showed the lowest values of $|Z|_{0.01\ Hz}$. The NaY containers loaded with the Ce^{3+} resulted in a significant increase of the $|Z|_{0.01\ Hz}$ of the gel-sol hybrid coatings, which indicates the formation of a stable oxide layer with higher resistance. Whereas the $|Z|_{0.01\ Hz}$ values of the hybrid sol-gel coatings loaded with LDH-MBT were in the same range as the NaY-Ce loaded coatings, containing NaY-Ce and LDH-MBT, showed the highest $|Z|_{0.01\ Hz}$ values that indicate synergy between the inorganic (Ce^{3+}) and organic (MBT) inhibitors in sol-gel hybrid coatings. Compared with the sol-gel hybrid coatings, the EIS spectra of the water-based epoxy coatings showed three specific time-constant after one-hour immersion in the electrolyte. This low coating resistance can be justified by poor LDH-MBT distribution, which disrupts the integrity of the coating due to the nanocontainer agglomeration. As a result of the poor barrier effect of the epoxy coating loaded with LDH-MBT, in the early stages of measurement, the low-frequency impedance ($|Z|_{0.01\ Hz}$) of this coating was also more than the coating loaded with NaY (Figure 4C). However, with the time progress and release of the encapsulate inhibitor, the coating loaded by LDH-MBT showed a higher $|Z|_{0.01\ Hz}$ values than the epoxy coating without container. The coating loaded with NaY-Ce showed the highest values of $|Z|_{0.01\ Hz}$ in the early stages of measurement, however, with the progress in immersion time, there was a sharp drop in $|Z|_{0.01\ Hz}$. The values of $|Z|_{0.01\ Hz}$ of the coating containing the combination of the inhibitors filled containers becomes a straight line after one day, that $|Z|_{0.01\ Hz}$ value exceeded than the $|Z|_{0.01\ Hz}$ values of NaY-Ce coating after immersion in the electrolyte for one week. The obtained results showed the improvement in the corrosion resistance of the coating when a combination of the filled inhibitors was used.

To measure the degree of inhibition and corrosion protection provided by the containers filled with inhibitors, the EIS spectra of the coating systems were fitted using equivalent circuits presented in Figure 5. In the equivalent circuits, R_{sol}, R_{coat}, $R_{oxide,}$ and R_{ct} are related to the resistance of solution, coating, oxide, and charge transfer, respectively. CPE_{coat}, CPE_{oxide}, and CPE_{dl} represent the constant phase element of the coating, oxide, and double layer, respectively [18, 19].

Figure 6 shows that the calculated resistances of the coating (R_{coat}) and the oxide (R_{oxide}) of the coating systems have a similar trend as Bode plot results at low frequencies, as shown in Figure 4. As can be seen in Figures 6A and 6C, the coating resistance related to both water-based epoxy coatings and sol-gel hybrid coatings decreased at the initial stage, and after that, the R_{coat} become constant. Thus, the R_{oxide} trend can provide a qualitative estimation of the performance of the container loaded with the inhibitor.

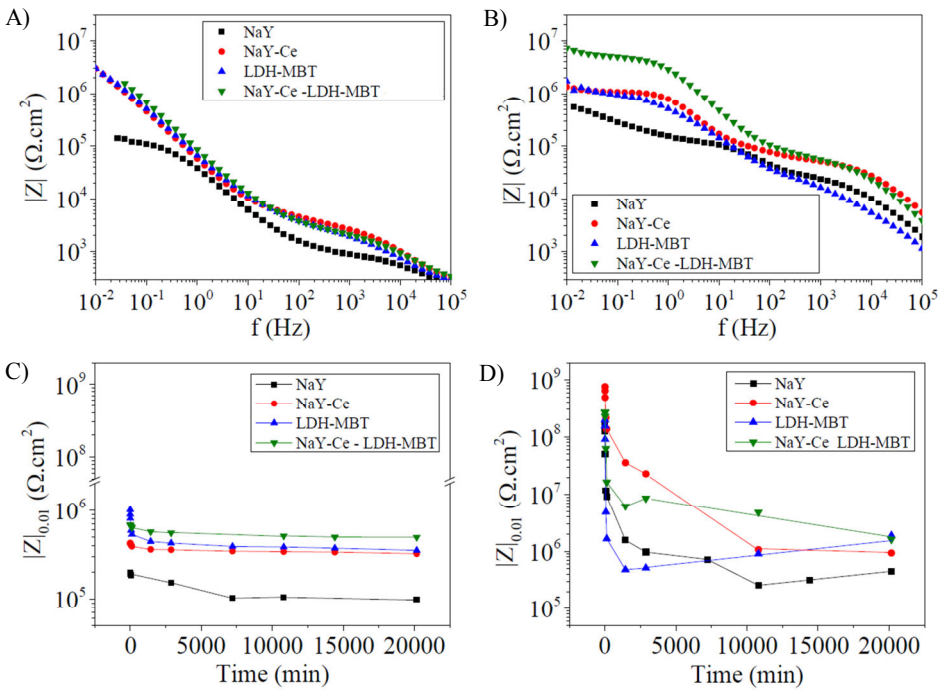

Figure 4: Bode plots and the related extracted data of SiO_2-ZrO_2 hybrid (Figure 4A and 4C) and water-based epoxy (Figure 4B and 4D).

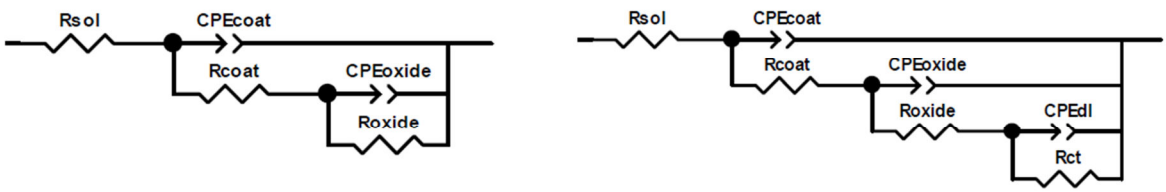

Figure 5: Equivalent circuits used for fitting of the EIS data.

The highest amount of R_{oxide} in the inhibitor filled container (NaY-Ce + LDH MBT) in sol-gel hybrid coatings during the measuring period (Figure 6B) and after passing 1 week of immersion for the water-based epoxy coatings (Figure 6D), reflecting the synergistic effect between these two inhibitors in the coating systems.

3.3. The corrosion inhibition mechanism of Ce^{3+}/2-mercaptobenzothiazole loaded NaY zeolite/Zn-Al LDH

The observed synergistic effect between the two inhibitor loaded containers not only can be attributed to the oxygen scavenging potential, but also ascribed to the stimuli-triggered release of the inhibitors from the containers. While the release of Ce^{3+} from NaY-Ce was boosted in acidic pHs, the release of MBT from LDH-MBT was amplified at basic/alkaline pHs. Therefore by using the combination of the inhibitor doped containers the release events can be expanded to a wide pH range (from very acidic to very basic) promoted by corrosion of AA2024-T3. The released inhibitors can subsequently deactivate the cathodic and anodic sites, restricting the Al dissolution rate. In contrary to the hybrid sol-gel coatings, the synergistic behavior of the two inhibitor loaded containers in the water-based epoxy coatings was only observed after 1 week of exposure to the electrolyte. At the early stages of the measurement, the R_{ct} of the NaY-Ce loaded coating was higher than the rest of the coating systems. Over time, the coating containing the combination of the inhibitor loaded container outperformed the NaY-Ce containing one.

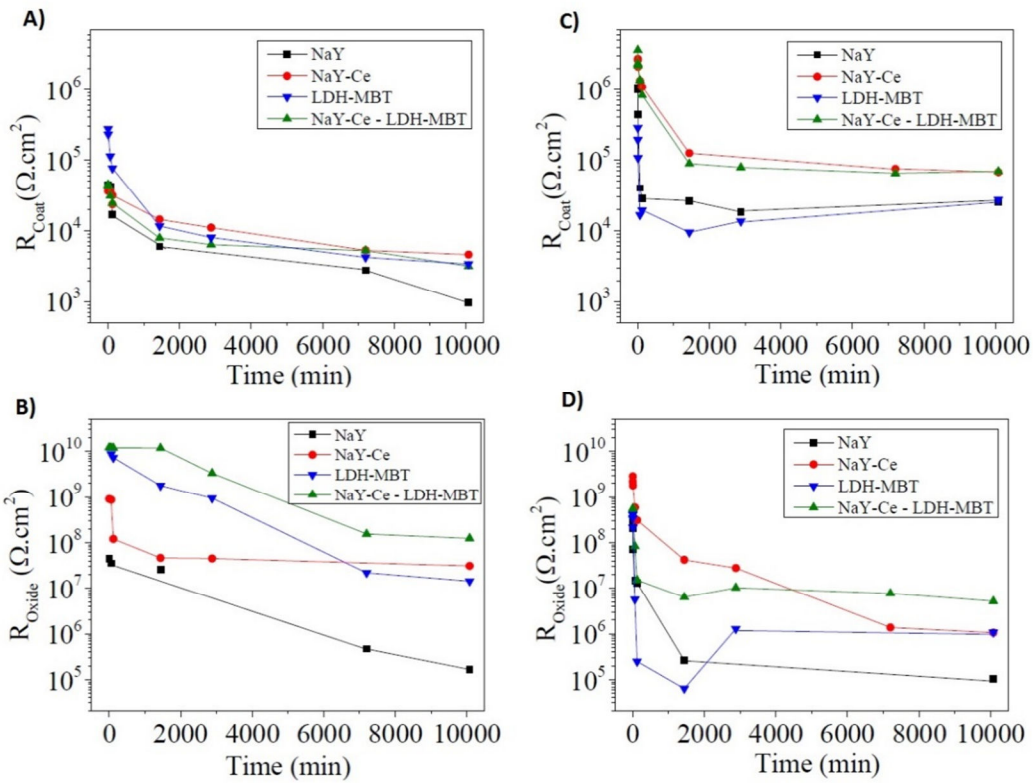

Figure 6: Resistances of the coating (R_{coat}) and oxide (R_{oxide}) of SiO_2-ZrO_2 hybrid (Figure 6A and 6B) and water-based epoxy (Figure 6C and 6D).

4. Conclusion

In this study, the preparation and evaluation of LDH containers and NaY zeolites loaded with inhibitor were explained. The Ce^{3+} and MBT were successfully loaded into LDH containers and NaY zeolites. The combination of the two inhibitors has a constructive effect on the active protection of AA2024-T3 sheets with a 1:1 ratio, which is the optimal molar ratio of Ce^{3+}: MBT. The addition of single-inhibitor filled containers to the sol-gel hybrid coating, and water-based epoxy coating provided active protection for the AA2024-T3 coated substrate. However, the combination of the filled containers with the inhibitor in the above-mentioned coatings resulted in the improvement of the active protection of the substrate, which confirms the synergy between them.

5. References

1. R. Amini, A. A. Sarabi, S. M. Kassiriha, Influence of sodium dodecyl sulfate on the structure and anti-corrosive properties of phosphate coating on AZ31 magnesium Alloy, *J. Color Sci. Technol*., 4(2010), 183-189.
2. R. Amini, H. Vakili, B. Ramezanzadeh, Studying the effects of poly (vinyl) alcohol on the morphology and anti-corrosion performance of phosphate coating applied on steel surface, *J. Taiwan Inst. Chem. Engrs*., 58(2016), 542-551.
3. M. L. Zheludkevich, Self-healing Anti-Corrosion Coatings in: S.K. Ghosh (Ed.) Self-Healing Materials: Fundamentals, Design Strategies, and Applications, Wiley-VCH, 2009.
4. Y Hayatgheib, B Ramezanzadeh, P Kardar, M Mahdavian, A comparative study on fabrication of a highly effective corrosion protective system based on graphene oxide-polyaniline nanofibers/epoxy composite, *Corr. Sci.*, 133(2018), 358-373.
5. B. Ramezanzadeh, P. Kardar, G. Bahlakeh, Y. Hayatgheib, M. Mahdavian, Fabrication of a highly tunable graphene oxide composite through layer-by-

layer assembly of highly crystalline polyaniline nanofibers and green corrosion inhibitors, *J. Phys. Chem.* C., 121(2017), 20433-20450.
6. D. W. Breck, Zeolite Molecular Sieves: Structure, Chemistry, and Use, (Union Carbide Corporation, Tarrytown, New York) John Wiley and Sons, New York, London, Sydney, and Toronto, 1984.
7. R. Xu, W. Pang, J. Yu, Q. Huo, J. Chen, Structural Chemistry of Microporous Materials, Chemistry of Zeolites and Related Porous Materials, John Wiley & Sons, Ltd. 2010, pp. 19-116.
8. S. A. S. Diasa, S. V. Lamakab, T. C. Diamantino, M. G. S. Ferreira, Synergistic Protection against Corrosion of AA2024-T3 by Sol-Gel Coating Modified with La and Mo-Enriched Zeolites, *J. Electrochem. Soc.*, 161 (2014), C215-C222.
9. H. Vakili, B. Ramezanzadeh, R. Amini, The corrosion performance and adhesion properties of the epoxy coating applied on the steel substrates treated by cerium-based conversion coatings, *Corr. Sci*., 94(2015), 466-475.
10. B. Ramezanzadeh, H. Vakili, R. Amini, Improved performance of cerium conversion coatings on steel with zinc phosphate post-treatment, *J. Ind. Eng. Chem*., 30(2015), 225-233.
11. E. Alibakhshi, E. Ghasemi, M. Mahdavian, B. Ramezanzadeh, A comparative study on corrosion inhibitive effect of nitrate and phosphate intercalated Zn-Al-layered double hydroxides (LDHs) nanocontainers incorporated into a hybrid silane, *Corr. Sci*., 115(2017), 225-233.
12. E. Alibakhshi, E. Ghasemi, M. Mahdavian, B. Ramezanzadeh, S. Farashi, Fabrication and characterization of PO43−intercalated Zn-Al-layered double hydroxide nanocontainer, *J. Electrochem. Soc*., 163(2016), C495-C505.
13. J. Tedim, S. Poznyak, A. Kuznetsova, D. Raps, T. Hack, M. Zheludkevich, M. Ferreira, Enhancement of active corrosion protection via combination of inhibitor-loaded nanocontainers, *Appl. Mater. Interfaces*, 2(2010) 1528-1535.
14. S. Poznyak, J. Tedim, L. Rodrigues, A. Salak, M. Zheludkevich, L. Dick, M. Ferreira, Novel inorganic host layered double hydroxides intercalated with guest organic inhibitors for anticorrosion applications, *Appl. Mater. Interfaces*. 1 (2009) 2353-2362.
15. K. Yasakau, S. Kallip, M. Zheludkevich, M. Ferreira, Active corrosion protection of AA2024 by sol–gel coatings with cerium molybdate nanowires, *Electrochim. Acta.*, 112(2013) 236-246.
16. E. L. Ferrer, A. P. Rollon, H. D. Mendoza, U. Lafont, S. J. Garcia, Double-doped zeolites for corrosion protection of aluminium alloys, *Micropor. Mesopor. Mat.*, 188 (2014) 8-15.
17. S. Garcia, T. Markley, J. Mol, A. Hughes, Unravelling the corrosion inhibition mechanisms of bifunctional inhibitors by EIS and SEM–EDS, *Corr. Sci.*, 69 (2013) 346-358.
18. S. Kallip, A. C. Bastos, K. A. Yasakau, M. L. Zheludkevich, M. G. Ferreira, Synergistic corrosion inhibition on galvanically coupled metallic materials, *Electrochem. Commun.*, 20 (2012), 101-104.
19. K. Aramaki, Effects of organic inhibitors on corrosion of zinc in an aerated 0.5 M NaCl solution, *Corr. Sci.*, 43 (2001), 1985-2000.

How to cite this article:
P. Kardar, R. Amini, Studying the Active Corrosion Inhibition Effect of the Ce^{3+}/2-Mercaptobenzothiazole Loaded NaY Zeolite/Zn-Al LDH Based Containers in a Silane Coating. Prog. Color Colorants Coat., 15 (2022), 1-9.